VOL. 10, NO. 1, JANUARY 2015 ISSN 1819-6608
ARPN Journal of Engineering and Applied Sciences


www.arpnjournals.com

PREDICTION OF NANOFILTRATION MEMBRANE PERFORMANCE: ANALYSIS OF ION TRANSPORT MECHANISMS

Norhaslina Mohd Sidek[1], Sarifah Fauziah Syed Draman[1], Nora'aini Ali[2] and Ilyani Abdullah[3]
[1]Faculty of Chemical Engineering, Universiti Teknologi Mara, Bukit Besi Campus, Dungun, Terengganu, Malaysia
[2]School of Ocean Engineering, Universiti Malaysia Terengganu, Kuala Terengganu, Terengganu, Malaysia
[3]School of Applied Informatics and Mathematics, Universiti Malaysia Terengganu, Kuala Terengganu, Terengganu, Malaysia
E-Mail: sfauziah@tganu.uitm.edu.my

ABSTRACT

The previous studies on nanofiltration (NF) more focusing on the work to update the existing predictive models to enhance its application in order to optimize the separation prediction. There is still lack of research which successfully assesses ion transport mechanisms modes for separation process prediction optimization. In this study, the percentage contribution of three transport modes: diffusion, electromigration and convection as described in Extended Nernst-Planck (ENP) equation were further evaluated. Prior the prediction, locally fabricated polysulfone (PSf) membranes with three different polymer concentrations; 19%, 21% and 23% were characterized in terms of pore radius, r_p ratio of membrane thickness to porosity, $\Delta x/A_k$ and effective charge density, X_d using uncharged and charged solutes rejection data, utilizing DSP prediction model in our developed NF-BIN system. The rejection prediction performance was then performed to predict the percentage contribution of ion transport mechanism at three cases; at limiting chloride ion rejections, at various r_p with constant ζ=3.5 and at various ζ with constant r_p=1.14 nm. The results obtained from this study indicated that diffusion is the most dominant and significant ion transport mode.

Keywords: nanofiltration; separation prediction; membrane characterization; transport model.

INTRODUCTION

Nanofiltration (NF) membranes, a relatively recent type of membranes, possess properties in between those of ultrafiltration (UF) and reverse osmosis (RO). The ionic transport mechanisms are therefore governed by both of steric and charge effects (Mohammad and Ali, 2002). This combined effect offers a value added to the membrane separation abilities, which covers almost all range of liquid-liquid separation system (Mohammad A.W. *et al.,* 2002). For all type of unit operation such as membrane separation system, having a good predictive tool is certainly vital in process performance prediction, hence, process design and optimization.

The ability to predict the performance of NF membrane separations is very important in the design and operation of processes. Such prediction requires a characterization of key membrane parameters (Mohammad and Takriff, 2003). NF membranes are normally characterized in terms of the structural parameters such as pore radius and membrane thickness as well as the electrical parameters such as charge density.

The assessment of the significance of each ion transport mechanisms in the NF membrane; diffusion, electromigration and convection are needed to comprehensively understand the ion transport behavior which would be very useful in improving the separation process. Literature shows lack of studies on the assessment of the ion transport mechanisms. In the preliminary stages, previous study successfully characterized and predicted the mechanisms for several commercial NF membranes and proved that each of the three modes of ion transport mechanism is significant (Bowen and Welfoor, 2002).

The next stage, investigation on the transport mechanisms shows that each mode of the mechanisms strongly influenced by membrane charge density, permeate volume flux, pore radius and effective membrane thickness to porosity ratio in determining the dominant modes at different operating conditions (Szymczyk *et al*., 2003).

The purpose of this paper is to assess and predict the in-house fabricated NF membrane separation behavior in terms of the percentage contribution of ion transport mechanisms by the means of diffusion, electromigration and convection upon NF membrane separation performance for binary salt solutions. It utilized DSP model for membrane characterization and separation performance prediction.

Theory of the Donnan Steric Pore model

Transport mechanisms of NF membrane were strongly influenced by both electrical (Donnan) and sieving (steric) effects. Combination of these two effects allows NF membranes to be effective for a range of separation of mixtures of organic and salts. Three main ion transportation mechanisms involved namely diffusion, electro-migration and convection, which entirely governed in extended Nernst-Planck equation (Eq. 1),

$$j_i = -D_{i,p}\frac{dc_i}{dx} - \frac{z_i c_i D_{i,p}}{RT} F \frac{d\varphi}{dx} + K_{i,c} c_i J \qquad \text{Eq. (1)}$$

Whereby j_i is flux of ion-*i*, $D_{i,p}$ is bulk diffusivity of ion-*i*, $K_{i,d}$ and $K_{i,c}$ are hindered factors for diffusion and convection respectively. This equation served as main components in Donnan Steric Pore (DSP) model. In order to obtain an expression for rejection of the solute, Eq. (1) is integrated across the membrane thickness with solute concentrations at the upper ($x=0$) and lower ($x=\Delta x$) surfaces expressed in terms of the external concentrations ($C_{i,x}$ and $C_{i,p}$) using the equilibrium partition coefficient, Φ:

$$\Phi = \frac{c_{i,x=0}}{C_{i,x}} = \frac{c_{i,x=\Delta x}}{C_{i,p}} = (1-\frac{r_s}{r_p})^2 \qquad \text{Eq. (2)}$$

Eq. (1) and Eq. (2) can be integrated and combined to give the following expression for calculating real rejection:

$$R_{real} = 1 - \frac{K_{i,c}\Phi}{1-\exp(-Pe_m)(1-\Phi K_{i,c})} \qquad \text{Eq. (3)}$$

Where the Peclet number, Pe_m, is defined as:

$$Pe_m = \frac{K_{i,c}}{K_{i,d}}\frac{V\Delta x}{D_{i,\infty}A_k} \qquad \text{Eq. (4)}$$

In the limiting case of the $Pe_m \to \infty$, the asymptotic rejection values (limiting rejection) will approach to $(1-\Phi K_{i,c})$. Thus, $(1-\Phi K_{i,c})$ represents a parameter of comparing the limiting rejection of solutes in membrane separation. The Hagen-Poiseuille equation relates the water flux to the applied pressure as well as r_p and $\Delta x/A_k$:

$$J_w = \frac{r_p^2 \Delta P}{8\mu(\Delta x / A_k)} \qquad \text{Eq. (5)}$$

Whereby J_w is flux of ion-*i*, r_p is membrane pore size, ΔP is operating pressure, $\Delta x/A_k$ is ratio of effective thickness to porosity, and μ is viscosity. Previous work has shown that Donnan exclusion and steric effects are significant in a small pore radii membrane, whereas steric hindrance is more prominent in relatively large pore radii membrane (Ali and Suhaimi 2009; Ali *et al*. 2005).

Once r_p and $\Delta x/A_k$ are obtained, the rejection data of NaCl can be used to estimate the effective charge density, X_d, of that particular membrane at the specified salt concentration using the transport model [8]. This value of X_d is specific for the specified NaCl concentration. Rejection data at different concentrations of NaCl is needed in order to obtain an isotherm that would be useful for predictive purposes at all salt concentrations, as has been shown in previous studies (Wang *et al.* 1995; Bowen and Mohammad, 1998; Bowen and Mokhtar, 1996)

Table-1. Main and supporting equations of DSP model.

Donnan Steric Pore model	
Potential gradient:	
$\frac{d\varphi}{dx} = \frac{\sum_{i=1}^{n}\frac{z_i J_V}{d_{i,p}}(K_{i,c}C_i - C_{i,p})}{\frac{F}{RT}\sum_{i=1}^{n} z_i C_i}$	Eq. (6)
Concentration gradient:	
$\frac{dc_i}{dx} = \frac{J_V}{D_{i,p}}(K_{i,c}C_i - C_{i,p}) - \frac{z_i c_i}{RT} F \frac{d\varphi}{dx}$	Eq. (7)
Donnan equilibrium:	
$\frac{c_i}{c_{i,w}} = \phi \exp -\frac{z_i F}{RT}\Delta\varphi_D$	Eq. (8)
where:	
$\phi = (1-\lambda)$	Eq. (9)
Electroneutralities equations:	
Boundary layer:	
$\sum_{i=1}^{n} z_i C_{i,w} = 0$	Eq. (10)
Membrane:	
$\sum_{i=1}^{n} z_i C_{i,w} = -X_d$	Eq. (11)
Permeate:	
$\sum_{i=1}^{n} z_i C_{i,p} = 0$	Eq. (12)
Hindrance factors:	
$K_{i,d} = K^{-1}(\lambda,0)$	Eq. (13)
$K_{i,c} = (2-\phi)G(\lambda,0)$	Eq. (14)
$D_{i,p} = K_{i,d} D_{i,\infty}$	Eq. (15)
$G(\lambda,0) = 1.0 + 0.054\lambda - 0.988\lambda^2 + 0.441\lambda^3$	Eq. (16)
$K^{-1}(\lambda,0) = 1.0 - 2.3\lambda + 1.154\lambda^2 + 0.224\lambda^3$	Eq. (17)

Ion Transport Mechanisms

In order to achieve the objective, the calculation of the contribution of each term in Eq. (1), the solution of

the equation has been approximated with a one-step central difference method [8]. Thus;

$$\frac{dc_i}{dx} = \frac{c_i(x=\Delta x) - c_i(x=0)}{\Delta x} \quad \text{Eq. (18)}$$

$$\frac{d\psi_m}{dx} = \frac{\psi_m(x=\Delta x) - \psi_m(x=0)}{\Delta x} \quad \text{Eq. (19)}$$

where $x=0$ indicates the membrane entrance and $x=\Delta x$ is the exit. The average concentration is defined as,

$$c_{i,avg} = \frac{c_i(x=\Delta x) - c_i(x=0)}{2} \quad \text{Eq. (20)}$$

Using the above equations, the contribution of each transport mechanism can be calculated and represented in terms of the percentage of the total contribution.

METHODOLOGY

The negatively-charged membranes made of polysulfone/N-methylpyrolidone/water with different of PSf concentration (19% w/w, 21% w/w and 23% w/w). Effective membrane area used in the experiment was 16.9 mm^2, and operating pressure of up to 10 bars. Glucose (MW=180), maltose (MW=342) and vitamin B12 (MW=1355) were chosen as neutral solutes, and Sodium chloride 0.01 M was used as the model for charged solutes. The experimental data were then incorporated into the predictive tools to obtain full range of fluxes and rejection.

The DSP model takes into account the transport across the entire mentioned medium such as hydrodynamic parameters, drag forces, lag coefficient etc. Bowen and Mokhtar, 1996). In this work, DSP model were utilized for binary solution (single salt solution) and the mathematical models were solved using MATLAB® m-file programming as has been shown in our previous work (Ali *et al.* 2014).

Three main ion transportation mechanism modes involved namely diffusion, electro-migration and convection, which entirely governed in ENP equation, Eq. (1). In order to achieve the research objective, the calculation of the contribution of each term in Eq. (1) is required.

The solution of the equation has been approximated with a one-step central difference method (Bowen and Mohammad, 1998) as described in Eqs. (18-20). Using the equations, the contribution of each transport mechanism mode can be calculated and represented in terms of the percentage of the total contribution.

RESULT AND DISCUSSIONS

Membrane Structural Parameters

The structural parameter values of locally made PSf membranes were within the range of reported values for commercially available membranes reported previously (Bowen and Mohammad, 1997; Kotrappanawar *et al.* 2011). Table-2 shows the P_m, r_p, X_d, $\Delta x/A_k$ and chlorides ion rejection values obtained from DSP model.

Table-2. Structural parameter details of PSF19, PSF21 and PSF23 membranes obtained from DSP model.

ID	P_m (L/m².h.bar)	r_p nm)	X_d (molm^{-3})	$\Delta x/A_k$	Limiting Cl^- ions Rejection (%)
PSF19	1.183	1.27	26.0	89.4	19.6
PSF21	0.521	1.14	35.0	130.5	38.7
PSF23	0.325	0.52	65.0	30.3	95.5

Assessment of Ion Transport Mechanism Modes at Limiting Chloride Ion Rejections

The ion transport modes analysis of three fabricated PSF membranes was performed at various r_p with constant ζ = 3.5 and various zeta with constant r_p = 1.14 nm.

As described in previous section, the contribution of each transport modes in the membrane can be calculated and represented in terms of percentage of the total contribution using Eqs. (18-20). The analysis has been carried out for NaCl and the solute flux (j_i) for Cl^- ion has been calculated in total and in its components using NF-BIN system. The data is represented as a function of flux.

The analysis has been carried for the fabricated PSf membrane using the data obtained in the characterization analysis. The limiting rejections were observed at J_v=50x10^{-6} m^3/m^2·s since the rejections

approached the maximum values at the selected flux. Tables 3-4 show the analysis of three fabricated PSF membranes at various r_p with constant $\zeta = 3.5$ and various zeta with constant $r_p = 1.14$ nm.

Table-3. Assessment of ion transport mechanisms percentage contribution for the PSF membranes at various r_p with constant $\zeta = 3.5$. ($J_{v,\,max} = 50\text{x}10^{-6}$ $m^3/m^2 \cdot s$).

r_p (nm)	R_{lim} of Cl^- ions (%)	Diffusion (%)	Electro-Migration (%)	Convection (%)
1.27	19.6	67.4	13.9	18.7
1.14	38.7	68.1	12.3	19.6
0.52	95.5	69.9	5.8	24.3

Table-4. Assessment of ion transport mechanisms percentage contribution for the PSF membrane at various ζ with constant $r_p = 1.14$ nm. ($J_{v,max} = 50\text{x}10^{-6}$ $m^3/m^2 \cdot s$).

ζ	R_{lim} of Cl^- ions (%)	Diffusion (%)	Electro-Migration (%)	Convection (%)
2.6	19.6	73.8	4.3	21.9
3.5	38.7	68.2	12.2	19.6
6.5	95.5	51.5	33.2	15.3

Inside the membrane, the diffusion, convection, and electromigration transport components of Cl^- ions will act towards the permeate side but for Na^+ ions only the diffusion and convection transport components are towards the permeate with the electromigration in the opposite direction (Mohammad *et al.* 2002).

All three transport mechanisms are seen to be significant at the limiting rejection. Elecromigration and convection show lower percentage contribution whilst convection exhibits the lowest measurement. Diffusion is likely to be the dominant mechanism involved for all the fabricated NF membranes with different structural parameters that strongly influences the separation behavior (Ali *et al.* 2014)] as described in Figure-1 and Figure-2. Transport is mainly governed by diffusion when the membrane is strongly charged; particularly at low permeate volume flux and effective membrane thickness to porosity ratio, $\Delta x/A_k$ (Szymczyk *et al.* 2003).

Assessment of Ion Transport Mechanism Modes at Constant Values of ζ

Figure-1 shows the analysis for three values of r_p for the constant value of ζ=3.5. The four boxes in the graph show the percentage rejection, and the percentage contributions of diffusion, convection, and the electromigration respectively.

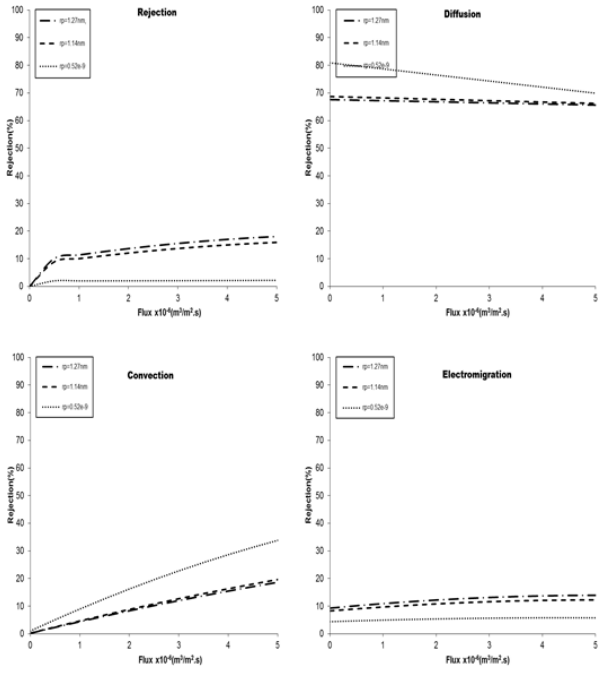

Figure-1. Result of effect of various r_p with constant ζ=3.5.

According to previous work (Bowen and Mohammad, 1998), this behavior would not have been expected if only the transport of Cl^- ions is considered because the diffusion, convection, and electromigration transport of Cl^- ions are moving in the direction of the permeate. However, for this constant value of ζ, the concentration of Na^+ is much larger than that of Cl^- inside the membrane. All three transport mechanisms are seen to be significant and diffusion exhibits the highest percentage contribution.

The percentage rejection, and the percentage contributions of each transport mechanism for r_p=1.27 nm and r_p=1.14 nm seem to be almost equal which indicates that the steric effect less influences the transport behavior as the pore size also almost equal. Besides, at r_p=0.52 nm, steric effect is the most prevailing as the pore size is the smallest.

Assessment of Ion Transport Mechanism Modes at Constant Values of r_p

Figure-2 illustrates the analysis for three values of ζ for the constant value of r_p=1.14 nm. At the largest values of ζ, the rejection is the highest and the transport is also controlled largely by diffusion mode. However, the contribution of convection can still reach 15-20% at the higher flux. For whole range of flux, the contribution of convection becomes equally significant for the three values of ζ. This phenomenon shows that Donnan effect less influences the percentage contribution of convection, contrast with the other two mechanisms.

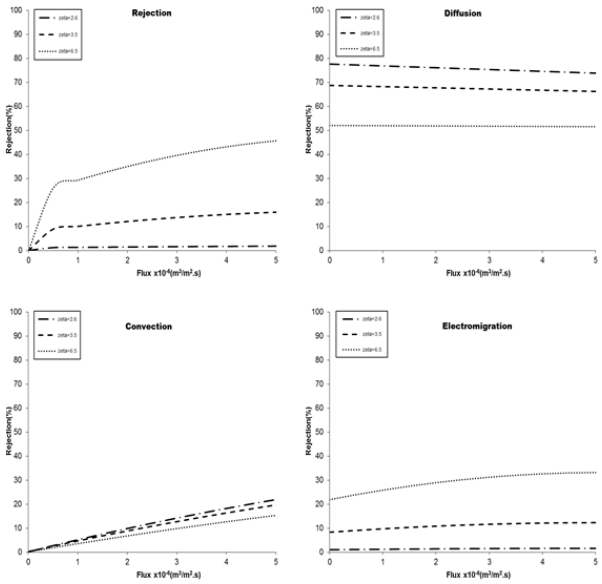

Figure-2. Result of effect of various ζ with constant r_p=1.14 nm.

CONCLUSIONS

For the range of r_p and ζ covered the analysis of ion transport modes, all the three transport modes play a significant role in the determination of ion rejections with diffusion is the most dominant mode. This finding has a good agreement with a recent study [15] which showed that the contribution of diffusive transport dominated at low flux, and convection and electromigrative transport, especially the latter, play an increasingly important role at a high flux.

Consequently, in order to optimize the separation process for engineering purposes, the diffusion should be further promoted by modifying the parameters governed in the diffusion mode to obtain the higher and optimum possible values.

It can be concluded that, an appropriate NF membrane specification for higher membrane separation performance could be predicted from the ion transport mechanisms analysis by means of the ion transport behavior details in terms of diffusion, electromigration and convection.

REFERENCES

A. Szymczyk, C. Labbez, P. Fievet, A. Vidonne, A. Foissy and J. Pagetti. 2003. Contribution of convection, diffusion and migration to electrolyte transport through nanofiltration membranes. Advances in Colloid and Interface Science. 103: 77-94.

A.W. Mohammad and M.S. Takriff. 2003. Predicting flux and rejection of multicomponent salts mixture in nanofiltration membrane. Desalination. 157: 105-111.

A.W. Mohammad and N.a. Ali. 2002. Understanding the steric and charge contributions in NF membranes using increasing MWCO polyamide membranes. Desalination. 147(1-3): 205-212.

A.W. Mohammad, L.Y. Pei and A.H. Khadum. 2002. Characterization and identification of rejection mechanisms in nanofiltration membranes using extended Nernst-Planck model. Clean Technology Environment Policy. 4: 151-156.

J. Fang and B. Deng. 2014. Rejection and modeling of arsenate by nanofiltration: Contributions of convection, diffusion and electromigration to arsenic transport. Journal of Membrane Science. 453: 42-51.

N.a. Ali, A.W. Mohammad, A.L. Ahmad. 2005. Use of nanofiltration predictive model for membrane selection and system cost assessment. Separation and Purification Technology. 41: 29-37.

N.a. Ali and N.S. Suhaimi. 2009. Performance Evaluation of Locally Fabricated Asymmetric Nanofiltration Membrane for Batik Industry Effluent. World Applied Sciences Journal, 5 (Special Issue for Environment). 46-52.

N.a. Ali, N.M. Sidek and I. Abdullah. 2014. Development of nanofiltration membrane separation prediction system for binary salt solutions. Desalination and Water Treatment Journal. 52: 626-632.

N.S. Kotrappanavar, A.A. Hussain, M.E.E. Abashar, I.S. Al-Mutaz, T.M. Aminabhavi, M.N. Nadagouda. 2011. Prediction of physical properties of nanofiltration membranes for neutral and charged solutes. Desalination. 280(1-3): 174-182.

W.R. Bowen and A.W. Mohammad. 1998. Characterization and prediction of nanofiltration membrane performance - A general assessment. Trans IChemE, 76 (Part A). 885-893.

W.R. Bowen and H. Mukhtar. 1996. Characterisation and prediction of separation performance of nanofiltration membranes. Journal of Membrane Science. 112(2): 263-274.

W.R. Bowen, A.W. Mohammad and N. Hilal. 1997. Characterisation of nanofiltration membranes for predictive purposes: use of salts, uncharged solutes and atomic force microscopy. Journal of Membrane Science. 126(1): 91-105.

W.R. Bowen and A.W. Mohammad. 1998. Diafiltration by nanofiltration: prediction and optimization, AIChE J. 44: 1799-1812.

W.R. Bowen and J.S. Welfoot. 2002. Predictive modelling of nanofiltration: membrane specification and process optimization. Desalination. 147(1-3): 197-203.

X.L. Wang, T. Tsuru, M. Togoh, S. Nakao and S. Kimura. Evaluation of pore structure and electrical properties of nanfiltration membranes, Jounal of Chem ical Engineering.

List of symbols

c_i	concentration in membrane (mol m^{-3})
$C_{i,b}$	concentration in the bulk solution (mol m^{-3})
$C_{i,p}$	concentration in permeate (mol m^{-3})
$C_{i,w}$	concentration at the membrane wall (mol m^{-3})
$D_{i,p}$	hindered diffusivity (m^2 s^{-1})
$D_{i,\infty}$	bulk diffusivity (m^2 s^{-1})
F	Faraday constant (C mol^{-1})
G	the hydrodynamic lag coefficient
K^{-1}	the hydrodynamic enhanced drag coefficient
j_i	ion flux (based on membrane area) (mol m^{-2} s^{-1})
$K_{i,c}$	hindrance factor for convection
$K_{i,d}$	hindrance factor for diffusion
P_m	membrane permeability (m^3 s^{-1} m^{-2} bar^{-1})
r_p	effective pore radius (m)
R	gas constant (J mol^{-1} K^{-1})
R_{real}	real rejection of the solute
T	absolute temperature (K)
x	distance normal to membrane (m)
Δx	effective membrane thickness (m)
X_d	effective membrane charge (mol m^{-3})
z_i	valence of ion
δ	thickness of film layer (m)
ΔP	applied pressure drop (bar)
Φ	coefficient as defined by Eq. (9)
$\Delta\psi$	potential difference (V)